PERGAMON

Journal of Structural Geology 25 (2003) 829–840

JOURNAL OF STRUCTURAL GEOLOGY

www.elsevier.com/locate/jsg

Separation of polyphase fault/slip data: an objective-function algorithm based on hard division

Yehua Shan[a,b,*], Hongbin Suen[b], Ge Lin[b]

[a]*Department of Marine Geology, Ocean University of Qingdao, 5 Yushan Road, Qingdao 266003, Shandong Province, People's Republic of China*
[b]*Changsha Institute of Geotectonics, Chinese Academy of Sciences, Changsha 410013, People's Republic of China*

Received 20 June 2002; accepted 24 June 2002

Abstract

The objective-function algorithm (OFA) on the basis of hard division is presented in the paper to separate polyphase fault/slip data. The separation is made by detection of linear structures existing in the data in Fry's (1999) sigma space. Different from other exhaustive-search methods, the OFA is direct and robust in theory without any arbitrary assumptions. Polyphase fault/slip data are simulated under prescribed tensors in order to validate the method. The results show its efficiency in stress estimation. The accuracy of stress estimation is controlled by random errors in the orientation of fault striations and by similarity between prescribed stress vectors related to different tectonic phases. The similarity between controlling stress vectors has an obvious effect on the estimation either when random errors are sufficiently large or when some similarity coefficients between the vectors are large enough. The accuracy of stress inversion tends to decrease as the range in errors increases. The OFA makes a very good approach to recognition of similar controlling stress vectors from polyphase fault/slip data, which are often associated with spatial and temporal variation of the tectonic stress field in a region, thus critical to understanding of the formation of geological structures.

Keywords: Stress inversion; Fault/slip data; Polyphase; Algorithm; Cluster analysis; Hard division

1. Introduction

Stress inversion from fault/slip data is an important technique in brittle tectonics for quantification of in-situ palaeostress states in the upper crust. Since the pioneering work of Carey and Brunier (1974), numerous methods have been developed to solve the inverse problem (Angelier, 1979, 1994; Etchecopar et al., 1981; Armijo et al., 1982; Huang, 1988; Fleischmann and Nemcok, 1991; Hardcastle and Hills, 1991; Nemcok and Lisle, 1995; Nemcok et al., 1999; Yamaji, 2000; Lisle et al., 2001). Existing methods can be roughly divided into two categories according to fault/slip data character. The first category assumes that fault/slip data are monophase, i.e. faults were active almost contemporaneously within a certain tectonic phase. The second category is concerned with the heterogeneity of fault/slip data, which can be formed as the response to multiple tectonic phases. It is known that faults in the brittle crust are weak zones that are frequently reactivated in subsequent stress fields (e.g. Nemcok et al., 1999). Therefore, polyphase fault/slip data are found more often than monophase fault/slip data in the field. When the polyphase nature of fault/slip data is not realized, the application of monophase methods undoubtedly leads to erroneous results.

In the case of polyphase fault/slip data, the critical task is how to separate the data into homogeneous subsets. Not all methods of the second category succeed in this task. Hardcastle and Hills (1991) utilized the exhaustive grid-search method to study the heterogeneity of fault/slip data. The fault/slip data are classified into a series of acceptable subsets, mutually dependent or independent, according to the deviation of the measured slip vectors of the faults from slip vectors calculated from the regularly chosen stress tensors. The tensor configuration that explains the largest percentage of data below the specified deviation threshold is considered the best-fit stress tensor and then taken as a criterion for separation of fault/slip data. This process is repeated until no best-fit tensor can be extracted from the remaining data. There is a drawback, however. Because the deviation threshold is the criterion for acceptance of a fault/slip datum into a subset related to a certain stress tensor,

* Corresponding author.
E-mail address: samscoun@public.qd.sd.cn (Y. Shan).

0191-8141/03/$ - see front matter © 2002 Elsevier Science Ltd. All rights reserved.
PII: S0191-8141(02)00082-2

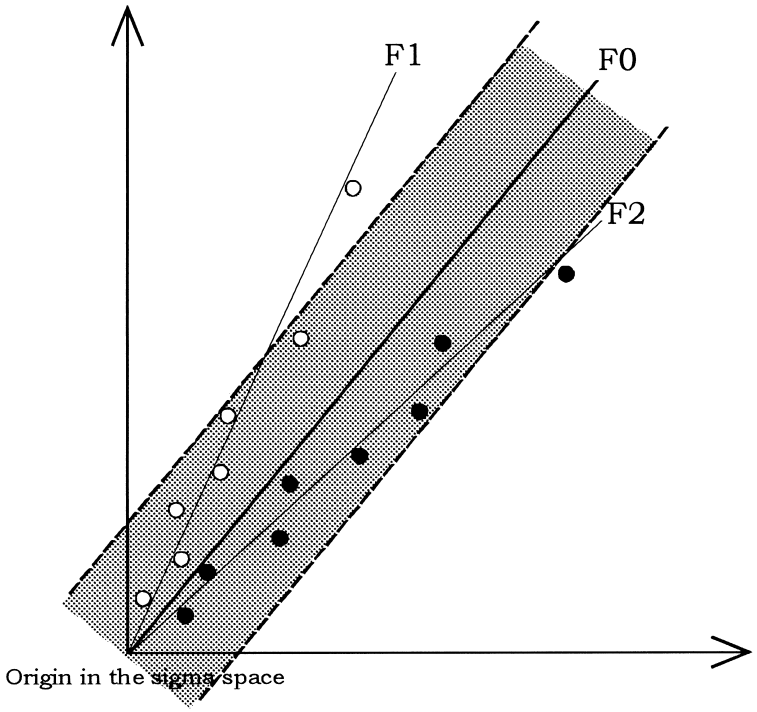

Fig. 1. A two-dimensional analogue of Fry's (1999) sigma space showing the failure in discrimination of a two-phase fault/slip data set. Unfilled and filled circles represent the fault/slip data related to F1 and F2 controlling stress tensors, respectively. The subset (grey area), related to a meaningless stress tensor F0, has the largest percentage of the data below the specified deviation threshold (dashed lines). The six-dimensional sigma space has orthogonal axes for the values of the six independent matrix elements σ_{11}, σ_{22}, σ_{33}, σ_{12}, σ_{13}, σ_{23} of the stress tensor.

there exists the possibility that it cannot separate heterogeneous data in which some or all of the controlling stress vectors are somewhat similar to each other in Fry's (1999) sigma space (Fig. 1). This means that the tensors obtained are likely to lie between real geological solutions (Will and Powell, 1991; Nemcok and Lisle, 1995; Nemcok et al., 1999). Furthermore, the role of the arbitrarily specified deviation threshold is like a filter on the separation. Too large or too low a value tends to lead to underestimation or overestimation of stress for polyphase fault/slip data. Optimization of the deviation threshold seems to be the best remedy to the routine, but has not attracted enough attention.

This intrinsic drawback is also found in other approaches, whether similar or different in philosophy. Nemcok and Lisle (1995) describe attributes of fault/slip data, relating them to a number of chosen stress tensors, and then apply an ordinary clustering method to group the data into subsets. The deviation threshold is still adopted in the definition of fault attributes. Its effect is difficult to decipher in subsequent grouping. However, we believe that the application of clustering analysis can help overcome the drawback to some degree, because the grouping or separation is based on similarity between the fault/slip data. Their approach is a comparatively good way for analysing the heterogeneity of fault/slip data.

However, Nemcok et al. (1999) expanded the above method recently. After separating fault/slip data in the same way, they replaced the classic inversion method by calculation of the orientation matrix defined on a stereonet by the right-dihedral solution for each separated fault/slip subset. The calculated orientation matrix is considered to correspond to the predicted stress tensor. This replacement makes it somewhat more convenient to see on a stereonet whether the separated fault/slip data is homogeneous or not. The same drawback still exists in their approach.

In his multiple inversion method Yamaji (2000) sampled, in a binomial pattern, *k*-element subsets from the fault/slip data set and calculated stress tensors of these subsets by the grid search method. He believed that the calculated tensors clustered around real stress states that he determined manually by projecting them onto the stereonet. This empirical assumption is valid for monophase data but lacks theoretical basis for polyphase data. In fact, there is a complex relationship between the clustering of calculated tensors and the fault/slip data. Apart from tectonic stresses and the number of fault/slip data in each phase, the sampling of the data is an important factor in controlling clustering. All these factors are commonly unknown for a fault/slip data set obtained in the field. It is thus imprudent to correlate the clustering of calculated tensors with controlling stress tensors for any fault/slip data set.

Other approaches include Simón-Gómez's (1986) Y–R diagram method, the backstripping method of Kleinspehn et al. (1989), Huang's (1988) method for Andersonian faults, etc. They all have limited application, and we do not discuss them here. Interested readers may look at the articles

of Nemcok and Lisle (1995) and Nemcok et al. (1999) for thorough reviews.

The nonlinear feature of stress inversion makes it rather complicated to calculate stress tensors directly from fault/slip data. This is probably the reason that some geologists even now prefer the 'direct' grid-search methods—an inefficiently global search in the parameter space—to 'indirect' numerical methods (Fleischmann and Nemcok, 1991). On the other hand, after some transformation, stress inversion can become a linear problem in which fault/slip data in response to the same tectonic phase will form a hyperplane or possess a linear structure in sigma space (Fry, 1999). The goal of our paper is to present an objective-function algorithm (OFA) on the basis of hard division. By utilizing modern clustering analysis (Bezdek, 1974, 1981), the method has the ability to separate polyphase fault/slip data by detecting linear structures existing in the data. It does not have the disadvantage of the deviation threshold in stress estimation. Polyphase fault/slip data are simulated for its validation (see later). By hard division we mean that a fault/slip data set can be divided into independent subsets, as do most existing methods. Otherwise it is called soft division (Guo and Zhuang, 1993).

2. New technique

2.1. Foundation

In inversion methods, the traction caused by stress difference on the fault plane is considered null in direction perpendicular to the striation (Angelier, 1979). It equals

$$n\sigma s^{\mathrm{T}} = 0 \tag{1}$$

where σ is the unknown stress tensor, n is the unit vector normal to the fault plane, s is the directional vector perpendicular to the fault striation within the fault plane and the superscript T is the operation of matrix transposition. Both n and s are derived from the fault/striation datum. Another geometrical meaning of Eq. (1) is that the fault slip recorded by the striation is parallel to the direction of maximum resolved shear stress on the fault plane. Other additional assumptions include independence between slips on different faults and homogeneity of the tectonic stress field (Carey and Brunier, 1974; Angelier, 1979; Etchecopar et al., 1981). These require that deformation recorded by faults be slight on a macroscopic scale (Twiss and Unruh, 1998). However, Wojtal and Pershing (1991) confirmed that it is also appropriate to apply inversion methods to intensively thrusted regions, which is attributed to low resistance to frictional sliding along the thrust surfaces and to material property without any memory of incremental stress in the process of large-offset thrusting.

Let us have a number N of fault/slip data in a single tectonic phase. Each fault/slip datum must satisfy Eq. (1). The misfit is caused by measurement errors. Accordingly, we have a number N of such linear equations for fault/slip data, which allows solving for stress tensor σ by the least squares method. However, these equations provide an infinite number of solutions because each reduced stress tensor is related to the full tensor by $\sigma_{\mathrm{full}} = PI + R\sigma_{\mathrm{reduced}}$ where $P$and R are any positive real numbers and I is the unit matrix (Angelier, 1979). Therefore, in order to reach a specific solution, additional constraints are required (modified after Fry, 1999):

$$\sum_{i=1}^{3} \sigma_{ii} = 0 \tag{2}$$

$$\frac{1}{2}\sum_{i=1}^{3}\sum_{j=1}^{3}\left(1+\delta(i,j)\right)\sigma_{ij}^{2} = 1 \tag{3}$$

where Kronecker delta $\delta(i,j)$ equals one when $i = j$ or zero when $i \neq j$. σ_{ij} is the element of stress tensor σ. Because of its symmetry, the nine unknown elements of the full tensor σ reduce to six unknown elements. And these constraints further reduce the parameter space from six to four dimensions without any distortion. In summary, Eqs. (1)–(3) constitute the basis of the stress inversion.

The left side of Eq. (1) may be rewritten as:

$$\sum_{i=1}^{3}\sum_{j=1}^{3} n_i\sigma_{ij}s_j = \sum_{i=1}^{3}\sum_{j=1}^{3}\left(n_i s_j\right)\sigma_{ij} = \sum_{i=1}^{3}\sum_{j=1}^{3} c_{ij}\sigma_{ij} \tag{4}$$

where $n = [n_1, n_2, n_3]$, $s = [s_1, s_2, s_3]$ and $c_{ij} = n_i s_j$. Because of symmetry of the stress tensor, it changes into:

$$\frac{1}{2}\sum_{i=1}^{3}\sum_{j=i}^{3}\left(2-\delta(i,j)\right)(c_{ij}+c_{ji})\sigma_{ij} \tag{5}$$

It is further modified by introducing the first constraint (Eq. (2)) to:

$$bt^{\mathrm{T}} = \sum_{i=1}^{5} b_i t_i \tag{6}$$

where $b = [b_1,\ b_2,\ b_3,\ b_4,\ b_5] = [c_{11}-c_{33},\ c_{22}-c_{33},\ c_{12}+c_{21},\ c_{13}+c_{31},\ c_{23}+c_{32}]$ and $t = [t_1,\ t_2,\ t_3,\ t_4,\ t_5] = [\sigma_{11}, \sigma_{22}, \sigma_{12}, \sigma_{13}, \sigma_{23}]$. b is the vector of fault/slip datum and t is the unknown stress vector in five dimensions.

Therefore, following Fry (1999), a concise formulation of Eq. (1) with the first constraint (Eq. (2)) is:

$$bt^{\mathrm{T}} = 0 \tag{7}$$

Eq. (7) has a distinct geometrical meaning. It states that the stress vector t is perpendicular to vectors of fault/slip data b,or that the Euler distance between the unknown stress vector and the five-dimensional stress plane with normal b is null. Because of the symmetry of stress tensor and the two constraints (Eqs. (2) and (3)), the parameter space is now a reduced sigma space. For convenience, we will make no distinction between them below. The second constraint (Eq.

Table 1
Fault/slip data in the example from Fry (1999)

No	Fault plane		Striation	
	Dip direction (°)	Dip angle (°)	Bearing (°)	Plunge (°)
1	283	86	12	18
2	110	35	20	6
3	89	32	9	7
4	147	36	200	15
5	45	47	328	13
6	360	90	270	8
7	50	66	325	12

(3)), is expressed in the unknown stress vector t as:

$$tt^{\mathrm{T}} = 1 \tag{8}$$

2.2. Objective function

The stress inversion can be defined as an optimum problem with a variety of corresponding algorithms. Here we define the objective function as the sum of the squares of the left side of Eq. (7). Assuming the homogeneity of fault/slip data, the objective function $F(t)$ becomes:

$$F(t) = \sum_{i=1}^{N} (b_i t)^2 = \sum_{i=1}^{N} t(b_i b_i^{\mathrm{T}})t^{\mathrm{T}} = \sum_{i=1}^{N} tA_i t^{\mathrm{T}}$$

$$= t\left(\sum_{i=1}^{N} A_i\right)t^{\mathrm{T}} = tAt^{\mathrm{T}} \tag{9}$$

where b_i is the stress vector related to the ith fault/slip datum, $A_i = b_i b_i^{\mathrm{T}}$, and A is the sum of A_i. Different from many inversion methods, our method builds on and provides a firmer mathematical justification of the method of Fry (1999), who referred to A as the second moment tensor and evaluated the eigenvector having the lowest eigenvalue. Our formulation optimizes the objective function under the constraint of Eq. (8). A variety of algorithms (Chen, 1996) can be used to solve the optimum problem. However, we propose a simple algorithm instead of these iterative algorithms (see Appendix B). In order to elucidate the competence of the algorithm, a data set from Fry (1999) is calculated (Table 1). It contains seven fault/slip measurements. Results from both Fry (1999) and us are listed in Table 2. There is only a slight difference between them.

When the fault/slip data are polyphase, the objective function $F(w,t)$ is defined as:

$$F(w,t) = \sum_{i=1}^{K}\sum_{j=1}^{N} w_{ij}t(i)A_j t(i)^{\mathrm{T}} \tag{10}$$

where K is the number of monophase subsets, w_{ij} is the characteristic parameter and $t(i)$ is the unknown stress vector for the ith subset. w_{ij} is defined as:

$$w_{ij} = \begin{cases} 0 & d_{ij} > d_j^* \\ 1 & d_{ij} = d_j^* \end{cases} \tag{11}$$

where d_{ij} is the Euler distance between the vector of the jth fault/slip datum b_j and the ith stress vector t_i, and d_j^* is the smallest Euler distance between the vector of the jth fault/slip datum b_j and the stress vectors. w_{ij} equals one when the jth datum belongs to the ith subset, or zero when it does not. Since w_{ij} discrete, equals zero or one, it is impossible for a fault/slip datum to belong to more than one subset. This algorithm is called hard division. It can be recasted to a soft division, in which w_{ij} may become any value between zero and one. This case requires an elaborate fuzzy clustering algorithm (Bezdek, 1974, 1981) for optimization (Shan et al., 2002). The soft division is beyond the scope of the paper.

2.3. Procedure

Both character parameters w and stress tensors t in the objective function (Eq. (10)) are unknown. They are obtained by minimizing the conditional objective function. The procedure to realize the OFA is as follows:

1. Set the division number K, or number of the monophase fault/slip subsets, which is more than one and usually smaller than six, select the initial division $w^{(0)}$ by random sampling for K homogeneous subsets, and let $i = 0$,
2. Apply the characteristic-equation method, which is described in Appendix B, in the division $w^{(i)}$ in order to optimize the stress vector $t^{(i)}$ for each subset,
3. Calculate $w^{(i+1)}$ for each fault/slip datum according to Eq. (11), and
4. Compare $w^{(i+1)}$ with $w^{(i)}$. If there is a difference between them, let $i = i + 1$ and return to step 2. If there is no difference, terminate the iteration and output the result.

Table 2
Comparison between Fry's (1999) result and our result. Stress ratio ϕ is defined as $(\sigma_1 - \sigma_2)/(\sigma_2 - \sigma_3)$

	σ_1		σ_2		σ_3		Stress ratio (ϕ)
	Azimuth (°)	Angle (°)	Azimuth (°)	Angle (°)	Azimuth (°)	Angle (°)	
Fry's result	359.00	2.00	263.00	73.00	90.00	17.00	4.00
Our result	1.00	1.09	267.01	74.70	91.30	15.26	3.83

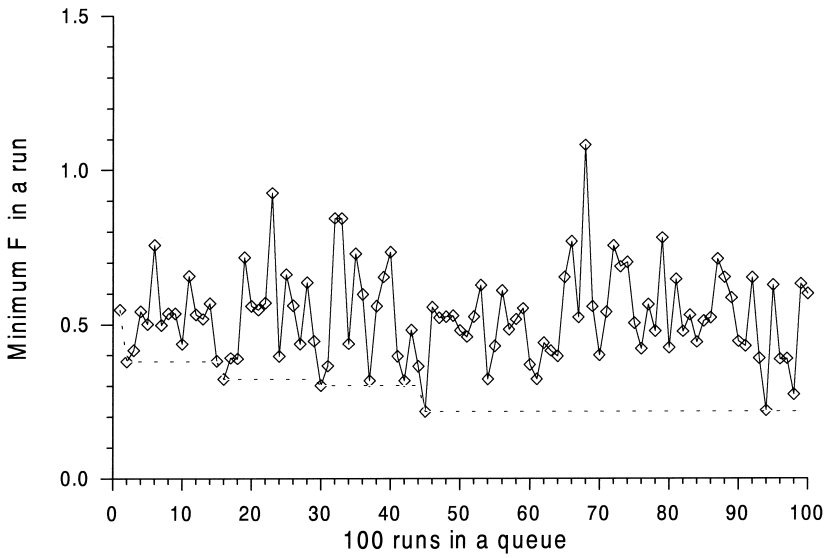

Fig. 2. Minimum values of the objective function F in 100 runs with different random seeds. Used fault/slip data are shown in case 2 in Fig. 3b. The number of subsets is three. Dashed line represents the least value of F at present runs. One hundred runs is large enough to find the least F that approximately equals 0.2.

The above algorithm is very effective and quick to converge. Sometimes the objective function may have a variety of local minima in the parameter space, and the final division is more or less related to the initial division (Guo and Zhuang, 1993). We do not have any good way to overcome a local minimum now. Our way is to perform a large number of runs, for example 100 (Fig. 2). Each has a different random seed. Then we select the one that has the least value of the objective function. The division of this run is considered to be the optimum one.

3. Test

In order to validate the use of OFA for solving for stress tensors, polyphase fault/slip data are simulated for numerically generated monophase sets. We make a validation set of polyphase fault/slip data consisting of three monophase subsets, each caused by stress with stress ratio of two (Table 3). For each tectonic phase, 20 fault/slip data are generated in two steps by Monte-Carlo sampling. In the first step, fault orientations are randomly selected from specific ranges, including fault dip directions ranging from 0° to 360° and dips from 45° to 85°. In the second step, the directions of maximum resolved shear on fault planes are calculated under the given stress tensor within each phase. Two different calculations were made. The second one incorporated simulated random errors into the fault/slip data, and the first one was exact. Therefore, for the OFA validation we have two sets of 60 artificial fault/slip data with monophase subsets related to three tectonic phases equally mixed (see Appendix C).

3.1. Case 1

Case 1 is an idealized polyphase data set, in which the orientation of simulated striation is strictly parallel to the direction of maximum resolved shear stress on the fault plane. Data are shown in Fig. 3a. The application of our OFA method to the simulated data (Appendix C) gave rise to results listed in Table 4.

Optimum stress tensors (Table 4) related to the division numbers, K, are compared with prescribed ones (Table 3). From this comparison it is apparent that calculated tensors are spurious for $K < 3$. Therefore it is dangerous to consider polyphase fault/slip data as monophase. The calculated tensor is almost meaningless in estimation except for representing some statistics of the data.

Table 3
Stress states of three prescribed tectonic phases. σ_1, σ_2 and σ_3 are the maximum, intermediate and minimum principal stresses, respectively. Stress ratio ϕ is defined as $(\sigma_1 - \sigma_2)/(\sigma_2 - \sigma_3)$.

Phase	σ_1		σ_2		σ_3		Stress ratio (ϕ)
	Azimuth (°)	Angle (°)	Azimuth (°)	Angle (°)	Azimuth (°)	Angle (°)	
1	180.00	10.00	89.00	5.65	329.93	78.48	2.00
2	140.00	5.00	235.00	44.89	45.04	44.67	2.00
3	100.00	1.00	195.00	78.67	9.80	11.28	2.00

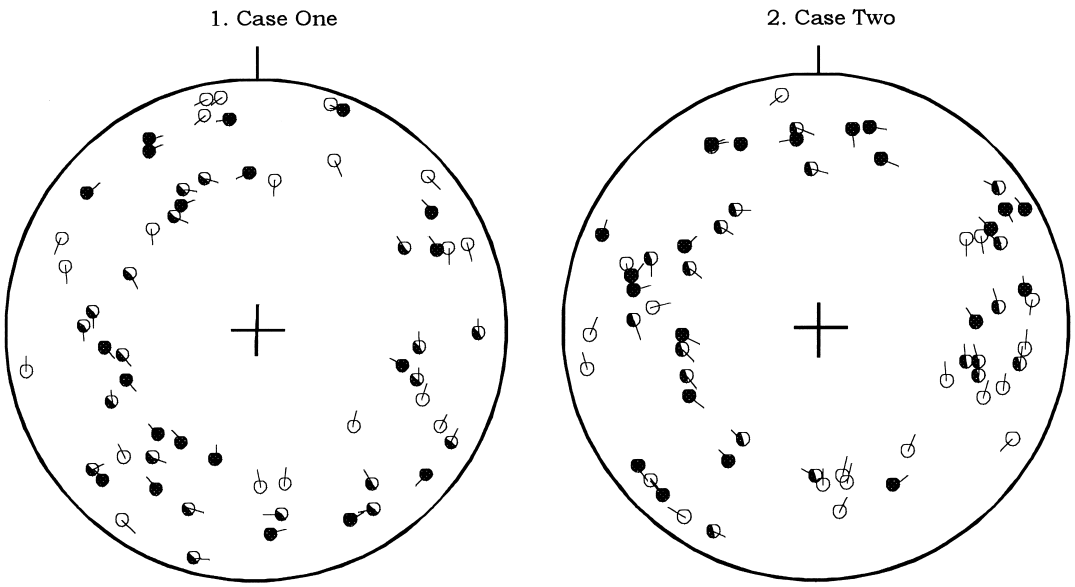

Fig. 3. Lower-hemisphere, equal-area projection of simulated polyphase fault/slip data listed in Appendix C. The fault striation is strictly parallel to the direction of maximum resolved shear on the fault plane in case 1, and subject to random deviations in case 2. Unfilled, half-filled and fully filled circles represent the normal to fault planes of the prescribed subsets 1, 2 and 3, respectively. Short lines represent plunges of the fault striations.

The minimum value of the objective function F decreases with K. It approximately equals zero when $K \geqq 3$. There is little difference in either orientation or in stress ratio between the prescribed and optimum stress tensors for $K \geqq 3$. Their divisions are exactly or almost identical to what we set before. This indicates that our method is able to separate polyphase fault/slip data and make the stress inversion. Furthermore, although F becomes less, a large subset number is not necessary for accurate estimation. For example, with K being five, the fourth optimum stress tensor is somewhat ambiguous in correlation. It probably reflects a subtle structure in the data that has nothing to do with prescribed stress tensors.

3.2. Case 2

This case represents a polyphase set in which not all orientations of the striations are exactly parallel to the direction of the maximum shear stress in the fault planes. The deviation from parallelism might be caused by such factors as measurement error, interaction between different faults and heterogeneity of the stress field. The latter two factors are in conflict with the assumptions of inversion methods. The striation plunge in case 2 is modified so as to simulate random errors in a range from $-5°$ to $5°$ (Fig. 3b). Random errors are considered to have an even distribution within the specific range. Results calculated from this data set (Appendix C) by our method are listed in Table 5.

Table 4
Estimation of stress tensors in case 1 with different division numbers (K). ϕ is the stress ratio and F is the minimum value of objective function

Division number (K)	Phase	σ_1		σ_2		σ_3		ϕ	F
		Azimuth (°)	Angle (°)	Azimuth (°)	Angle (°)	Azimuth (°)	Angle (°)		
1	1	165.45	3.94	257.49	27.32	67.89	62.35	1.95	5.70
2	1	148.27	16.22	244.25	19.70	21.57	64.03	3.08	1.61
	2	82.35	13.34	196.18	59.60	345.48	26.77	1.79	
3	1	180.00	10.00	89.00	5.65	329.94	78.48	2.00	1.6×10^{-7}
	2	140.00	5.00	235.00	44.89	45.04	44.68	2.00	
	3	100.00	1.00	194.99	78.67	9.80	11.28	2.00	
4	1	180.00	10.00	89.00	5.65	329.94	78.48	2.00	0.0×10^{-7}
	2	140.00	5.00	235.00	44.89	45.04	44.68	2.00	
	3	100.00	1.00	194.99	78.67	9.80	11.28	2.00	
	4	0.00	0.00	0.00	0.00	0.00	0.00	0.00	
5	1	180.00	10.00	89.00	5.65	329.94	78.48	2.00	0.0×10^{-7}
	2	140.00	5.00	235.00	44.89	45.04	44.68	2.00	
	3	100.00	1.00	194.99	78.67	9.80	11.28	2.00	
	4	307.84	4.13	58.49	78.42	217.05	10.80	1.95	
	5	0.00	0.00	0.00	0.00	0.00	0.00	0.00	

Table 5
Estimation of stress tensors in case 2 with different division numbers. See Table 4 for explanation

Division number (K)	Phase	σ_1		σ_2		σ_3		ϕ	F
		Azimuth (°)	Angle (°)	Azimuth (°)	Angle (°)	Azimuth (°)	Angle (°)		
1	1	158.69	4.94	252.05	34.11	61.48	55.4	1.08	5.16
2	1	319.31	24.96	228.16	2.48	132.84	64.90	0.28	1.12
	2	145.18	28.87	253.38	29.53	19.84	46.37	0.22	
3	1	182.37	22.43	89.29	7.41	342.09	66.25	0.72	2.2×10^{-1}
	2	312.58	7.08	217.52	35.36	52.32	53.72	3.66	
	3	212.56	0.08	302.61	33.03	122.44	56.97	0.08	
4	1	174.97	11.34	269.03	19.45	56.39	67.26	3.10	1.1×10^{-1}
	2	139.65	2.93	232.60	45.12	46.74	44.73	1.70	
	3	356.14	24.87	91.66	11.73	204.81	62.15	0.09	
	4	285.62	2.82	188.41	68.62	16.71	21.18	0.83	
5	1	10.33	24.55	220.39	62.17	106.04	12.28	5.54	5.1×10^{-2}
	2	140.63	10.55	239.96	41.06	39.11	47.01	1.17	
	3	179.21	11.12	88.93	1.43	351.69	78.79	2.28	
	4	315.62	36.46	218.96	8.92	117.32	52.11	0.31	
	5	172.51	26.56	265.08	5.13	5.18	62.87	1.32	

Comparison of results with those in case 1 (Table 4) shows that the decrease of the F value with K is quite small (Table 5). For example, for $K = 5$, F reaches 0.0×10^{-7} in case 1 and only 5.1×10^{-2} in case 2. The optimum stress tensors differ more from prescribed ones, and become more difficult to correlate. Calculated optimum divisions in the case 2 data set are not satisfactory. For $K = 3$ just 50% or a little more of the data fits the category of prescribed subsets (Table 6).

Evidently, the introduction of random errors into the orientation of fault striations gives rise to the low accuracy of stress estimation. The least value of the objective function tends to increase with the range of errors (Fig. 4). Additionally, the similarity between prescribed stress vectors is another factor that must be taken into consideration. Random errors, on their own, generally cause approximately the same accuracy of estimation of the different controlling tensors. But this is far from what we expect (Table 5), which implies the influence of one or more other factor. In the presence of errors in the data, the more similar are the prescribed vectors and the greater is the possibility of misallocation of a fault/slip datum to a prescribed subset; thus the less accurate tends to be the estimation of the controlling stress vectors. Similarity coefficients between the three prescribed stress vectors are listed below:

$$\begin{array}{l} \text{Stress vector 1} \\ \text{Stress vector 2} \\ \text{Stress vector 3} \end{array} \begin{bmatrix} 1.000 & 0.812 & 0.673 \\ 0.812 & 1.000 & 0.904 \\ 0.673 & 0.904 & 1.000 \end{bmatrix}$$

The similarity coefficient between prescribed stress vectors 2 and 3 reaches the maximum, 0.904, and that between prescribed stress vectors 1 and 3 reaches the minimum, 0.673. Their effect on the estimation is therefore obvious, especially for a relatively large range of errors in data (Fig. 4). It is interesting to note that the prescribed vector 1 is somewhat distinct for relatively low similarity coefficients between it and other vectors, so that the accuracy of its estimation becomes relatively high (Table 6).

4. Discussion

In essence the OFA on the basis of hard division is a peculiar recast of fuzzy clustering algorithms of Bezdek (1974, 1981). Therefore, it is different from other inversion methods designed for polyphase data separation. The OFA is the most direct way we know for analyzing the heterogeneity of fault/slip data. The goal is completed by

Table 6
Comparison between divisions in cases 1 and 2, both with a division number of three

Prescribed subsets	Optimum subsets in case 1				Optimum subsets in case 2			
	1	2	3	Total number	1	2	3	Total number
1	20	0	0	20	13	0	7	20
2	0	20	0	20	4	10	6	20
3	0	0	20	20	4	8	8	20
Total number	20	20	20	60	21	18	21	60
Percentage	33.33	33.33	33.33	100.00	35.00	30.00	35.00	100.00

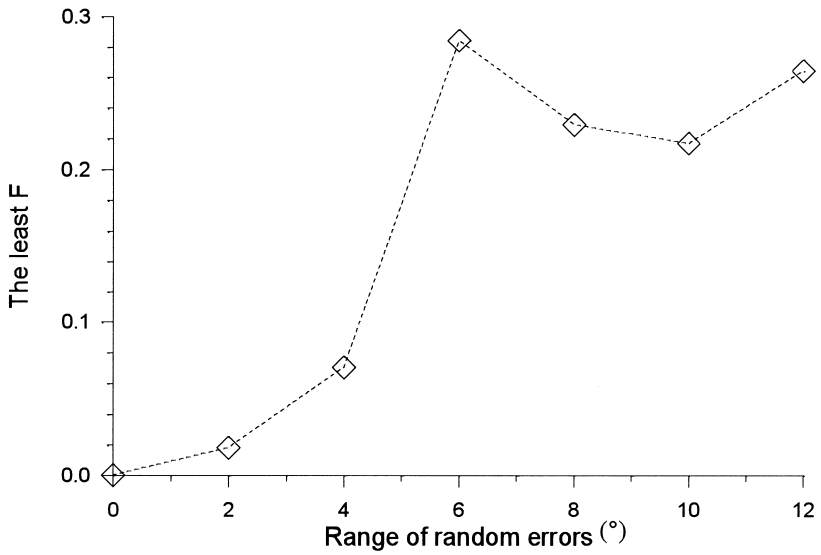

Fig. 4. The least value of the objective function F versus the range of random errors in plunges of striations. Division number is three. The smaller the range of errors the smaller the value of F is likely to be.

detection of linear structures existing in the data in Fry's (1999) sigma space. Variables in the OFA, including stress vectors and data division, are solved in iteration. And the run is relatively fast. On this point, we dare to say the OFA is robust in theory. Except for the assumptions necessary for stress inversion, it is free from other assumptions or limits, for example the deviation threshold for accepting a fault/slip datum into a certain subset related to a given stress tensor. As shown in Fig. 1, the disadvantage of the threshold used in grid-search methods (Hardcastle and Hills, 1991) is that it is often inappropriate or even invalid for the polyphase data in which some or all similarity coefficients between the controlling stress vectors are large in sigma space. That is to say, subtle tectonic stresses may not be recognized through grid-search methods. In contrast, the OFA makes a very good approach to stress inversion from fault/slip data of this kind. Its failure in stress estimation is not due to its theory but due to the data. It is able in most cases to recognize subtle tectonic stresses that are often associated with spatial and temporal variation of the tectonic stress field in a region, which is important to understanding the formation of geological structures.

However, the drawback of the OFA is sometimes its low efficiency in overcoming local minimum in the presence of large random errors in the data. At present we have no good way but to make many runs and choose the least one. In our test we have confirmed that 100 runs are sufficient (Fig. 2), but we are not sure whether there exists a minimum number of runs for any fault/slip data set or not. Fewer runs might not be enough for successful data separation and for calculation of controlling stress tensors, and more runs take a lot of time. Moreover, neither slip sense nor frictional law is included in the method. Because of this, our OFA method needs further improvement.

As shown in the test, the OFA is competent in separating polyphase fault/slip data into monophase subsets. The accuracy of stress estimation is controlled by errors in the orientation of fault striations and by similarity between prescribed stress vectors of different tectonic phases. The method is particularly efficient if fault striations are strictly or approximately parallel to the direction of maximum resolved shear on fault planes. Optimum stress tensors are apparently in good agreement with prescribed ones in this case. However, if random errors are included in the orientations of fault striations, optimum tensors become inconsistent with prescribed ones. Size of the random errors is closely associated with the accuracy of stress estimation (Fig. 4). This effect is especially obvious in the case when some or all controlling stress vectors are mutually similar. This further implies that only the field data related to distinct tectonic phases are easy to separate. We believe that this is a common problem for all inversion methods for polyphase data sets.

The effect of similarity of the different prescribed stress vectors on the accuracy of stress estimation remains rather unclear if errors exist in the data. The more similar the controlling stress vectors the less accurate the estimation. It is frustrating to note that no exact solution exists to deal with this problem because we have no prior knowledge about the intrinsic deviation from linear structures in fault/slip data. The only way to try this now is to combine other geological data into the analysis. Field data similar to case 2 require that calculated stress tensors should be carefully interpreted and only those consistent with other geological data accepted with confidence.

Acknowledgements

This research was supported by the CAS program

(KZCX2-113) and the Shandong NSF (Grant Y98E08078). Most of the work was done in "Laboratory for Numerical Simulation of Continental Deformation and Dynamics" in the Changsha Institute of Geotectonics, Chinese Academy of Sciences. We thank N. Fry, M. Nemcok, C. Liesa and A. Nieto-Samaniego for their critical reviews, useful suggestion and substantial improvement of the written English.

Appendix A

List of symbols and their definitions

Symbol	Definition	Comment
σ	Stress tensor	See Eqs. (1) and (A1)
σ_{ij}	The element of the stress tensor, $i,j = 1,2,3$	See Eqs. (3)–(5) and (A2)–(A5)
σ_{full}	Full stress tensor	
σ_{reduced}	Reduced stress tensor	
n	The unit vector normal to the fault plane	See Eqs. (1) and (A1)
n_i	The element of the vector n, $i = 1,2,3$	See Eqs. (4) and (A2)
s	The directional vector perpendicular to the fault striation	See Eqs. (1) and (A1)
s_i	The element of the vector s, $i = 1,2,3$	See Eqs. (4) and (A2)
c_{ij}	$c_{ij} = n_i s_j$, $i,j = 1,2,3$	See Eqs. (4), (5) and (A2)
t	The stress vector	See Eqs. (6)–(9) and (A5)–(A12)
t_i	The element of the vector t, $i = 1,2,\ldots,5$	See Eqs. (6) and (A5)
$t(i)$	The ith stress vector, $i = 1,2,\ldots,K$	See Eq. (10)
t^*	The optimum stress vector for a monophase fault/slip data set	See Eq. (A12)
b	The vector of fault/slip datum	See Eqs. (6), (7), (A5), (A6) and (A8)
b_i	The element of the vector b, $i = 1,2,\ldots,5$	See Eqs. (6), (A5) and (A8)
$b(i)$	The vector of the ith fault/slip datum, $i = 1,2,\ldots,N$	See Eqs. (9) and (10)
N	The number of fault/slip data	
K	The division number	
P and R	Any two real positive numbers	
I	A 3×3 unit matrix	
A_i	The matrix for the ith fault/slip datum, $i = 1,2,\ldots,N$	See Eqs. (9), (10) and (A8)
A	The sum of A_i, $i = 1,2,\ldots,N$	See Eqs. (9), (A8) and (A10)–(A12)
W_{ij}	The characteristic parameter, $i = 1,2,..,K$, $j = 1,2,\ldots,N$	See Eqs. (10) and (11)
$\delta(i,j)$	Kronecker delta, one when $i = j$ or zero when $i \neq j$	See Eqs. (3), (5), (A4) and (A5)
d_{ij}	The Euler distance between the vector b_j and the stress vector t_i, $i = 1,2,..,K$, $j = 1,2,\ldots,N$	See Eq. (11)
d_j^*	The smallest Euler distance between the vector b_j and the stress vector, t, $j = 1,2,\ldots,N$	See Eq. (11)
$F(t)$	The objective function for monophase fault/slip data	See Eqs. (9), (A8) and (A9)
$F(w,t)$	The objective function for polyphase fault/slip data	See Eq. (10)
λ	The Lagrange parameter or the eigenvalue	See Eqs. (A9)–(A12)
λ^*	The least eigenvalue	See Eq. (A12)
$P(t,\lambda)$	The composite objective function	See Eqs. (A9) and (A10)

Appendix B. Algorithm for monophase fault/slip data

One of the fundamental assumptions of stress inversion is the parallelism of the fault slip to the direction of maximum resolved shear stress on the fault plane (Angelier, 1979):

$$n\sigma s^{\mathrm{T}} = 0 \tag{A1}$$

where σ is the stress tensor, n is the unit vector normal to the fault plane, $n = [n_1, n_2, n_3]$, s is the directional vector perpendicular to the fault striation within the fault plane, $s = [s_1, s_2, s_3]$, and the superscript T is the operation of matrix transposition. The left side of Eq. (A1) is rewritten as:

$$\sum_{i=1}^{3}\sum_{j=1}^{3} n_i\sigma_{ij}s_j = \sum_{i=1}^{3}\sum_{j=1}^{3}\left(n_i s_j\right)\sigma_{ij} = \sum_{i=1}^{3}\sum_{j=1}^{3} c_{ij}\sigma_{ij} \tag{A2}$$

where $c_{ij} = n_i s_j$.

Let us have a number N of fault/slip data in a single tectonic phase. We have a number N of such Eq. (A1), one for each datum. Because these equations are not enough to make a specific resolution, additional constraints are required to reduce the parameter space (modified after Fry, 1999):

$$\sum_{i=1}^{3}\sigma_{ii} = 0 \tag{A3}$$

$$\frac{1}{2}\sum_{i=1}^{3}\sum_{j=1}^{3}\left(1+\delta(i,j)\right)\sigma_{ij}^2 = 1 \tag{A4}$$

where Kronecker delta $\delta(i,j)$ equals one when $i = j$ or zero when $i \neq j$. σ_{ij} is the element of stress tensor σ.

Because of the symmetry of stress tensor, Eq. (A2) is further modified to:

$$\frac{1}{2}\sum_{i=1}^{3}\sum_{j=i}^{3}\left(2-\delta(i,j)\right)(c_{ij}+c_{ji})\sigma_{ij}$$

which with the first constraint (Eq. (A3)) leads to:

$$bt^{\mathrm{T}} = \sum_{i=1}^{5} b_i t_i \tag{A5}$$

where $b = [b_1, b_2, b_3, b_4, b_5] = [c_{11}-c_{33}, c_{22}-c_{33}, c_{12}+c_{21}, c_{13}+c_{31}, c_{23}+c_{32}]$ and $t = [t_1, t_2, t_3, t_4, t_5] = [\sigma_{11}, \sigma_{22}, \sigma_{12}, \sigma_{13}, \sigma_{23}]$. b is the vector of fault/slip datum and t is the unknown stress vector in five dimensions.

Therefore, Eq. (A1) with the inclusion of the first constraint (Eq. (A3)) is expressed as (Fry, 1999):

$$bt^{\mathrm{T}} = 0 \tag{A6}$$

The expected stress vector t is five-dimensional and perpendicular to vectors of fault/slip data.

In terms of stress vector, the second constraint (Eq. (A4) is rewritten as:

$$tt^{\mathrm{T}} = 1 \tag{A7}$$

In order to make stress inversion, we define the objective function, $F(t)$, as the sum of the squares of the left side of Eq. (A6):

$$F(t) = \sum_{i=1}^{N}(b_i t)^2 = \sum_{i=1}^{N} t(b_i b_i^{\mathrm{T}})t^{\mathrm{T}} = \sum_{i=1}^{N} tA_i t^{\mathrm{T}}$$

$$= t\left(\sum_{i=1}^{N} A_i\right)t^{\mathrm{T}} = tAt^{\mathrm{T}} \tag{A8}$$

where b_i is the stress vector related to the ith fault/slip datum, $A_i = b_i b_i^{\mathrm{T}}$, and A is the sum of A_i. The matrix A_i is symmetrical by its definition, so the sum, matrix A, is also. Thus, stress inversion becomes optimization of the objective function with one constraint (Eq. (A7)). Instead of optimum methods (Chen, 1996), we use the characteristic-equation method for the conditional minimization. It is derived by introducing a new composite objective function $P(t,\lambda)$, in which the constraint is included:

$$\min P(t,\lambda) = F(t) - \lambda(tt^{\mathrm{T}} - 1) \tag{A9}$$

where λ is the Lagrange parameter. The routine way to solve it is to set the partial derivatives from $P(t,\lambda)$ null and then solve these equations. The partial derivative of t from $P(t,\lambda)$ is:

$$\frac{\partial P(t,\lambda)}{\partial t} = 2tA - 2\lambda t \tag{A10}$$

Let it be zero. After division it becomes:

$$tA = \lambda t \tag{A11}$$

where λ is also called the eigenvalue. This is a characteristic equation and might be solved in numeric methods such as the Jacobi method (Agterberg, 1974; Yuan et al., 1992). Let λ^* and t^* be the least eigenvalue and its corresponding eigenvector. Inserting them into Eq. (A9) results in:

$$P(t^*,\lambda^*) = t^*At^{*\mathrm{T}} - \lambda^*(t^*t^{*\mathrm{T}} - 1)$$

$$= (\lambda^* t^*)t^{*\mathrm{T}} - \lambda^*(t^*t^{*\mathrm{T}} - 1) = \lambda^* \tag{A12}$$

The function $P(t,\lambda)$ has a positive quadratic form. It can be proven (Xue and Pei, 1994) that the value of $P(t^*,\lambda^*)$ reaches the minimum. Therefore, t^* is the optimum stress vector which we search for.

Appendix C. Simulated fault/slip data with monophase subsets related to three tectonic phases (Table 3)

No.	Case 1				Subset	Case 2				Subset
	Fault plane		Striation			Fault plane		Striation		
	Dip direction (°)	Dip angle (°)	Plunge (°)	Pitch (°)		Dip direction (°)	Dip angle (°)	Plunge (°)	Pitch (°)	
1	348.70	53.07	12.57	50.58	1	348.7	53.07	12.8	50.53	1
2	187.03	50.29	183.08	50.22	1	47.61	79.97	132.39	79.93	1
3	314.71	45.98	9.88	30.59	1	171.21	83.05	240.77	70.77	1
4	171.21	83.05	242.94	68.76	1	276.96	72.57	5.19	5.63	1
5	114.77	75.77	191.80	41.51	1	108.1	69.88	175.05	46.91	1
6	248.12	80.16	163.02	26.22	1	240.95	63.67	185.09	48.59	1
7	108.10	69.88	171.13	51.07	1	79.71	83.33	352.18	20.29	1
8	297.41	71.77	24.89	7.62	1	349.33	50.17	7.95	48.65	1
9	168.00	83.45	244.98	62.98	1	358.47	52.72	0.96	52.69	1
10	79.71	83.33	351.57	15.54	1	240.35	59.89	180.97	41.3	1
11	198.42	83.81	116.79	53.33	1	293.17	61.96	11.97	20.03	1
12	46.56	63.03	330.31	25.03	1	288.66	67.76	12.18	15.43	1
13	358.47	52.72	358.73	52.72	1	34.96	82.94	305.94	82.94	1
14	246.74	71.71	172.07	38.65	1	323.83	50.54	21.88	32.74	1
15	134.04	48.05	173.25	40.76	1	352.78	63.02	18.83	60.46	1
16	293.17	61.96	12.43	19.28	1	88.14	80.93	10.55	53.41	1
17	166.10	77.07	228.18	63.89	1	299.83	79.35	215.6	28.1	1
18	204.86	63.42	162.51	55.90	1	263.15	75.77	192.84	53.03	1
19	34.96	82.94	124.33	5.11	1	96.07	56.59	74.56	54.66	1
20	228.33	80.98	143.72	30.60	1	292.1	47.27	356.54	25.03	1
21	49.90	76.45	56.68	76.36	2	143.81	46.97	109.41	41.48	2
22	352.78	63.02	274.87	22.36	2	91.22	62.86	168.36	23.48	2
23	63.44	54.79	342.53	12.62	2	79.76	46.24	148.81	20.47	2
24	323.39	66.23	327.55	66.18	2	111.55	61.87	168.22	45.79	2
25	299.83	79.35	25.29	22.85	2	287.47	57.06	353.8	31.77	2
26	327.23	74.24	263.93	57.86	2	134.53	46.72	126.07	46.41	2
27	276.96	54.21	349.59	22.49	2	112.99	46.6	134.6	44.51	2
28	96.07	56.59	165.02	28.57	2	173.53	67.33	105.78	42.2	2
29	271.07	77.46	356.88	18.17	2	245.83	68.73	320.44	34.28	2
30	20.39	65.22	106.69	7.96	2	0.97	50.06	298.9	29.23	2
31	143.81	46.97	114.10	42.94	2	69	46.84	144.78	14.68	2
32	39.19	55.14	116.56	17.43	2	280.12	71.22	4.68	15.58	2
33	160.78	52.74	107.32	38.05	2	149.2	73.08	84.7	54.77	2
34	79.76	46.24	146.77	22.18	2	263.87	61.5	338.22	26.41	2
35	241.13	57.39	319.57	17.40	2	33.43	45.52	307.83	4.46	2
36	151.84	53.15	108.02	43.92	2	282.65	54.21	348.38	29.69	2
37	287.47	57.06	356.78	28.59	2	283.4	50.31	356.45	19.36	2
38	90.64	59.95	168.70	19.66	2	232.76	79.55	304.65	59.31	2
39	15.48	84.16	103.17	21.56	2	177.36	52.57	107.54	24.26	2
40	112.99	46.6	139.51	43.42	2	26.65	82.07	114.88	12.49	2
41	32.73	64.28	310.61	15.9	3	42.64	80.38	318.33	30.35	3
42	201.01	84.11	290.02	9.49	3	51.5	80.79	140.17	80.79	3
43	245.83	68.73	329.19	16.54	3	113.14	83.93	27.05	32.7	3
44	17.74	45.11	339.85	38.38	3	173.35	64.49	254.49	17.9	3
45	45.57	74.89	316.66	4.05	3	237.92	78.05	149.52	78.04	3
46	69	46.84	131.8	25.98	3	334.47	60.21	57.48	11.99	3
47	129.16	76.12	43.73	17.87	3	101.25	64.53	76.71	62.36	3
48	235.96	73.44	323.1	9.52	3	33.16	54.02	317.37	18.69	3
49	149.2	73.08	61.92	8.88	3	194.33	72.7	107.93	11.41	3
50	172.74	74.32	262.6	0.52	3	201.29	61.95	120.07	15.98	3
51	148.49	48.38	65.16	7.45	3	86.3	45.19	119.79	40.01	3
52	33.43	45.52	316.44	12.91	3	156.9	68.07	73.05	14.91	3
53	150.32	76.41	62.34	8.29	3	240.22	83.76	327.48	23.62	3
54	82.86	51.05	126.78	41.71	3	60.96	48.46	135.16	17.09	3
55	283.4	50.31	281.89	50.3	3	190.12	69.13	166.86	67.46	3
56	355.58	70.86	74.94	28.03	3	240.32	67.32	318.73	25.69	3
57	310.93	77.83	222.29	6.28	3	121.39	52.16	59.61	31.33	3
58	177.36	52.57	245.82	25.63	3	105.71	66.3	55.53	55.57	3
59	43.14	47.96	314.5	1.51	3	260.37	73.62	339.42	32.86	3
60	333.6	73.6	62.19	4.78	3	267.62	53.47	321.85	38.27	3

References

Agterberg, F.P., 1974. Geomathematics, Mathematical Background and Geoscience Applications, Elsevier Scientific Publishing Company, Amsterdam.

Angelier, J., 1979. Determination of the mean principal directions of stresses for a given fault population. Tectonophysics 56, T17–T26.

Angelier, J., 1994. Fault slip analysis and palaeostress construction. In: Hancock, P.L., (Ed.), Continental Deformation, Pergamon Press, London, pp. 53–100.

Armijo, R., Carey, E., Cisternas, A., 1982. The inverse problem in microtectonics and separation of tectonic phase. Tectonophysics 82, 145–160.

Bezdek, J.C., 1974. Cluster validity with the fuzzy sets. Journal of Cybernetics 3, 58–73.

Bezdek, J.C., 1981. Detection and characterization of clustering algorithms. II. Journal of Applied Mathematics 40, 21–33.

Carey, M.E., Brunier, M.B., 1974. Analyse theorique et numerique d'un modele mecanique elementaire applique a l'etude d'une population de failes. Compte Rendus Hebdomadaires des Seances de l'Academie des Sciences 279, 891–894.

Chen, B., 1996. Optimum Theory and its Algorithms, Qinghua University Press, Beijing, (in Chinese).

Etchecopar, A., Vasseur, G., Daignieres, M., 1981. An inverse problem in microtectonics for the determination of stress tensors from fault striation analysis. Journal of Structural Geology 3, 51–65.

Fleischmann, K.H., Nemcok, M., 1991. Paleostress inversion of fault/slip data using the shear stress solution of Means (1989). Tectonophysics 196, 195–202.

Fry, N., 1999. Striated faults: visual appreciation of their constraint on possible palaeostress tensors. Journal of Structural Geology 21, 7–22.

Guo, G., Zhuang, Z., 1993. Fuzzy Techniques in Information Processing, Press of National Defense University of Science and Technology, Changsha, (in Chinese).

Hardcastle, K.C., Hills, L.S., 1991. Brute3 and Select: Quickbasic 4 programs for determination of stress tensor configurations and separation of heterogeneous. Computer and Geosciences 17, 23–43.

Huang, Q., 1988. Computer-based method to separate heterogeneous sets of fault-slip data into subsets. Journal of Structural Geology 10, 297–299.

Kleinspehn, K., Pershing, J., Teyssier, C., 1989. Palaeostress stratigraphy: a new technique for analyzing tectonic control on sedimentary-basin subsidence. Geology 17, 253–257.

Lisle, R.J., Orife, T., Arlegui, L., 2001. A stress inversion method requiring only fault slip sense. Journal of Geophysical Reaserch 106, 2281–2289.

Nemcok, M., Lisle, R.J., 1995. A stress inversion procedure for polyphase fault/slip data sets. Journal of Structural Geology 17, 1445–1453.

Nemcok, M., Kovac, D., Lisle, R.J., 1999. Stress inversion procedure for polyphase calcite twin and fault/slip data sets. Journal of Structural Geology 21, 597–611.

Shan, Y., Li, Z., Lin, G., 2002. A stress inversion procedure for automatic recognition of polyphase fault/slip data sets. Acta Geoscientia Sinica, in press (in Chinese with English abstract).

Simón-Gómez, J.L., 1986. Analysis of a gradual change in stress regime: example from the eastern Iberian Chain. Tectonophysics 124, 37–53.

Twiss, R.J., Unruh, J.R., 1998. Analysis of fault slip inversions: do they constrain stress or strain rate? Journal of Geophysical Research 103, 12205–12222.

Will, T.M., Powell, R., 1991. A robust approach to the calculation of paleostress fields from fault plane data. Journal of Structural Geology 13, 813–821.

Wojtal, S., Pershing, J., 1991. Paleostress associated faults of large offsets. Journal of Structural Geology 13, 49–62.

Yamaji, A., 2000. The multiple inverse method: a new technique to separate stresses from heterogeneous fault-slip data. Journal of Structural Geology 22, 441–452.

Yuan, W., Zhang, L., Huang, X., Wen, Z., 1992. Numerical Analysis, Southeastern University Press, Nanjing, (in Chinese).

Xue, Zh., Pei, Y., 1994. Fundamentals of Mathematical Geology, Beijing University Press, Beijing, (in Chinese).